A Novel Parallel Pinching and Self-adaptive Grasping Robotic Hand

Dayao Liang and Wenzeng Zhang(✉)

Department of Mechanical Engineering,
Tsinghua University, Beijing 100084, China
wenzeng@tsinghua.edu.cn

Abstract. This paper introduces a novel underactuated hand, the PASA-GB hand which has a hybrid grasping mode. The hybrid grasping mode is a combination of parallel pinching (PA) grasp and self-adaptive enveloping (SA) grasp. In order to estimate the performance of grasping objects, the potential energy method is used to analyze the stabilities of the PASA-GB hand. The calculation of force distribution shows the influence of the size and position of objects and provides a method to optimize the force distribution. Experimental results verify the wide adaptability and high practicability of the PASA-GB hand.

Keywords: Robot hand · Underactuated finger · Parallel and self-adaptive grasp · Grasping stability

1 Introduction

Robotic hands have been highly researched for decades. As the end effectors, robotic hands accomplish most of the missions for robots. Traditional robot hand have many joints, the number of which is the same as degrees of freedom (DOFs). They are dexterous hands such as DLR-HIT Hand [1], Robonaut 2 hand [2], Gifu hand II [3], Belgrade/USC Hand [4], NAIST Hand [5]. Although dexterous hands are flexible, the establishment of control systems and sensor systems are difficult. In common cases, the actuators have to be small to set inside the phalanges. As a result, the grasping forces are small. Industrial grippers [6] successfully deal with these difficulties, but most of them have only one DOF.

Underactuation was proposed to handle the contradiction between high DOFs and large grasping force. Underactuated hands use less actuators to control more DOFs with special mechanisms. The control problem is changed to the design problem of the mechanisms, as the mechanisms determine the behaviors and grasping stabilities of the finger. Outstanding designs include: Underactuated hand: MARS hand [7], bio-mimetic robot hands [8], prosthetic FDD-hand [9], pneumatically driven TWIX-hand [10], FRH-4 hand [11], and soft gripper [12]. Methods to optimize the performance of underactuated hand [13, 14] were also proposed.

However, the grasping modes of traditional underactuated hands are single. In order to perform more grasping modes, people developed hybrid grasping mode hand: such as Barrett Hand grasper [15], SARAH hand [16], and Robotiq hand [17].

A. Agah et al. (Eds.): ICSR 2016, LNAI 9979, pp. 469–480, 2016.
DOI: 10.1007/978-3-319-47437-3_46

This paper introduces a novel parallel and self-adaptive robot hand with gear-belt mechanisms (PASA-GB hand), which possesses the advantages of large grasping force and multiple grasping modes. It combines the good qualities of dexterous hands, underactuated hands and industrial grippers. The second part introduces the architecture of the PASA-GB hand, the third part analyzes the stability and force distribution of the PASA-GB hand, the forth part shows the experimental results, the fifth part concludes this paper.

2 Architecture of the PASA Hand

2.1 Concept of Parallel and Self-adaptive Underactuated Grasp

Parallel pinching grasp is a common grasping mode for traditional industrial gripper. It is the most appropriate way to grasp some specially objects, such as paper, which needs precise grasp [18]. However, Enveloping grasp is more tightly for large objects than pinching grasp, as enveloping grasp is often power grasp. In order to combine the advantages of both pinching grasp and enveloping grasp, [19] introduces the concept of parallel and self-adaptive underactuated finger and introduced a PASA finger with belt-link mechanism.

As it is shown in Fig. 1, parallel and self-adaptive underactuated (PASA) grasping mode is a hybrid grasping mode. Based on the location, size and shape of objects, a parallel and self-adaptive underactuated finger (PASA finger) executes parallel pinching motion if the lower part of the finger touches the objects first, or executes enveloping grasp if the higher part touches the objects first. Because of the special mechanisms of PASA finger, the switch among different grasping modes is automatic and self-adaptive.

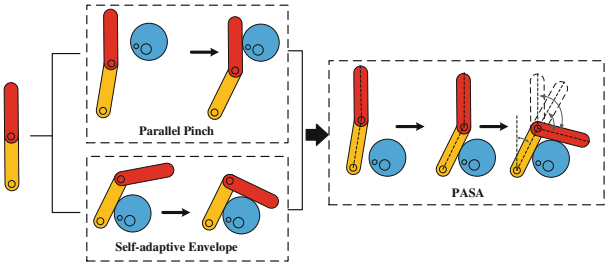

Fig. 1. Concept of parallel and self-adaptive underactuated grasp.

2.2 Mechanisms and Structure of the PASA Hand

The PASA finger mainly consists of a finger base, a proximal phalanx, a distal phalanx, a proximal joint, a distal joint, a driving gear, a driven gear, a gear set, a proximal wheel, a distal wheel, a transmission belt, a sliding block, a spring, a motor and a limiting block, as it is shown in Fig. 2.

The transmission belt links the proximal wheel and the distal wheel, which are in the same size. The distal phalanx is fixed to the driven gear, which is fixed to the distal wheel and driven by the driving gear through the gear set. The transmission ratio between the driving gear and the driven gear is a. The sliding block is set on the proximal wheel. The spring links the sliding bock and the finger base and drives the proximal wheel rotating backwards. The limiting block is set on the finger base and limits the backward motion of the proximal wheel.

At the beginning, the sliding block abuts the limiting block, which makes the proximal wheel "fixed" to the finger base. Because of the transmission belt, the distal wheel can only translate without rotation on condition that sliding block doesn't leave the limiting block. As a result, the distal phalange executes parallel pinching motion.

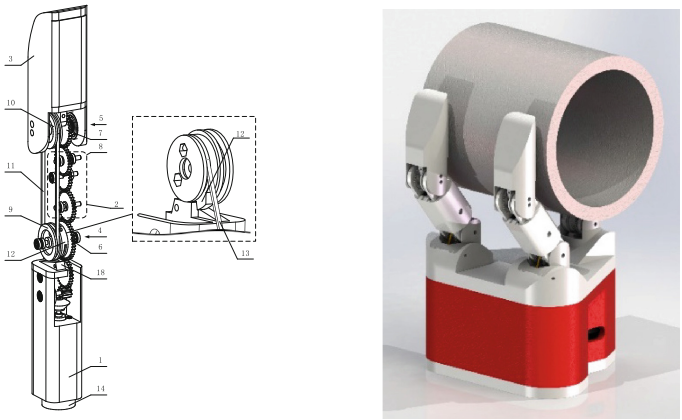

Fig. 2. Mechanisms and structure of the PASA-GB hand. 1-Finger base, 2-Proximal phalanx, 3-Distal phalanx, 4-Proximal joint, 5-Distal joint, 6-Driving gear, 7-Driven gear, 8-Gear set, 9-Proximal wheel, 10-Distal wheel, 11-Transmission belt, 12-Sliding block, 13-Spring, 14-Motor, 18-Limiting block

Let θ_1 be the rotational angle of the proximal phalanx, θ_2 be the rotational angle of the distal phalanx, and β the rotational angle of the driving gear. Referencing to the proximal phalanx, the rotational angle of the driving gear is $\beta - \theta_1$, that of the driven gear is $\theta_2 - \theta_1$. The transmission ratio between the driving gear and the driven gear is a, one achieves

$$a(\beta - \theta_1) = \theta_2 - \theta_1, \tag{1}$$

The rotational angle θ_1 can be described as follow:

$$\theta_1 = a\beta/(a - 1), \tag{2}$$

It means that, when the driving gear moves forwards, the proximal phalanx rotates with a proportionate speed to the driving gear.

Once the proximal phalanx is blocked by objects, the driving gear continues rotating and drives the distal wheel rotating through the gear set. The rotational angle of the distal phalanx is

$$\theta_2 = a\beta - \theta_1(a-1), \tag{3}$$

As a result, the rotational speed of the distal phalanx is also propionate to the driving gear. Because the proximal wheel rotates, the sliding block has to leave the limiting block and the spring is strained. Such motion is self-adaptive enveloping grasp.

3 Analysis of the PASA Hand

This part focuses on the analyses of stability, force distribution and switch condition among different grasping modes. For the reason of simplification, the contact forces are considered as point forces, the friction and gravity are neglected.

3.1 Stability Analyses

This part analyzes the stability of the PASA-GB hand. Stability is one of the most important performance for robot hands [20]. Because the number of actuators is less than the degrees of freedom (DOFs), stability is difficult to gain by the control systems. Therefore, the analyses of stability and optimization of parameters of the PASA-GB finger are important.

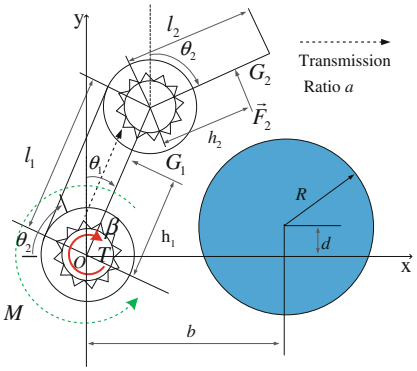

Fig. 3. Stability analyses of the PASA-GB finger.

As Fig. 3 shows, O is the center point of the proximal joint axis, l_1, l_2 are the length of the proximal phalanx and the distal phalanx, G_1, G_2 are the contact points between phalanges and objects, h_1, h_2 are the distances between the joint axis and contact

points, $\vec{F}_1$, $\vec{F}_2$ are the external force vectors produced by objects, M is the value of the spring torque, T is the value of the driving torque.

Because of the transmission belt, the rotational angles of the proximal wheel and the distal phalanx are the same. Let M_0 be the initial spring torque when $\theta_2 = 0$, so can be defined as $M = k\theta_2 + M_0$, where k is the elastic coefficient of the spring.

To simplify the problem, the object is considered as a column, of which the radius is R. Set up a rectangular coordinate system at the point O, the coordinate of the center of the object is (b, d).

$\vec{P}_1$ and $\vec{P}_2$ are points on the proximal phalanx and distal phalanx

$$\vec{P}_1 = (H_1 \sin\theta_1, H_1 \cos\theta_1),\ 0 \le H_1 \le l_1, \tag{4}$$

$$\vec{P}_2 = (l_1 \sin\theta_1 + H_2 \sin\theta_2, l_1 \cos\theta_1 + H_2 \cos\theta_2),\ 0 \le H_2 \le l_2, \tag{5}$$

When the proximal phalanx touches the object, the slope of proximal phalanx can be obtained by simple calculation:

$$k_1 = \pm\frac{R\sqrt{-R^2 + b^2 + d^2} - bd}{\sqrt{R^2 - b^2}}, \tag{6}$$

At this moment, the rotational angle of the proximal phalanx is

$$\theta_{10} = \operatorname{atan}\left(\pm\frac{\sqrt{R^2 - b^2}}{R\sqrt{-R^2 + b^2 + d^2} - bd}\right), \tag{7}$$

The distance h_1 can be obtained by geometry relation:

$$h_1 = \frac{d + b\tan\theta_{10}}{\cos\theta_{10} + \tan\theta_{10}\sin\theta_{10}}, \tag{8}$$

When the distal phalanx touches the object, the slope of distal phalanx is:

$$k_2 = \frac{S \pm R\sqrt{-R^2 + (b - l_1\sin\theta_1)^2 + (d - l_1\cos\theta_1)^2}}{R^2 - (b - l_1\sin\theta_1)^2}, \tag{9}$$

Where, $S = bl_1\cos\theta_1 - bd + dl_1\sin\theta_1 - l_1^2\cos\theta_1\sin\theta_1$

And the rotational angle of the distal phalange is

$$\theta_{2c} = \operatorname{atan}\left(\frac{R^2 - (b - l_1\sin\theta_1)^2}{S \pm R\sqrt{-R^2 + (b - l_1\sin\theta_1)^2 + (d - l_1\cos\theta_1)^2}}\right), \tag{10}$$

The distance between the contact point on the distal phalanx and the distal joint

$$h_2 = \frac{-l_1(\tan\theta_{2c}\sin\theta_1 + \cos\theta_1) + b\tan\theta_{2c} + d}{\cos\theta_{2c} + \tan\theta_{2c}\sin\theta_{2c}}, \tag{11}$$

If both the proximal phalanx and distal phalanx touch the object,

$$\theta_{20} = \text{atan}\left(\frac{R^2 - (b - l_1\sin\theta_{10})^2}{Y \pm R\sqrt{-R^2 + (b - l_1\sin\theta_{10})^2 + (d - l_1\cos\theta_{10})^2}}\right), \tag{12}$$

Where, $Y = bl_1\cos\theta_{10} - bd + \mathrm{d}l_1\sin\theta_{10} - l_1^2\cos\theta_{10}\sin\theta_{10}$

In order to analyze the stability of grasp, one introduces the potential energy V, which is produced by the driving torque T and the spring torque M:

$$V = \phi - T\beta + \frac{1}{2}k\theta_2^2 + M_0\theta_2, \tag{13}$$

where ϕ is potential energy of the PASA-GB finger in the initial state.

The condition for complete stable enveloping grasp is when both phalanges touch the object, the potential energy V reaches the minimum point.

In arbitrarily states, β can be described as

$$\beta = \frac{\theta_1(a-1)}{a} + \frac{\theta_2}{a}, \tag{14}$$

One achieves

$$V = \phi - T\frac{(a-1)}{a}\theta_1 + \frac{1}{2}k\theta_2^2 + (M_0 - \frac{T}{a})\theta_2, \tag{15}$$

When θ_1 increases, should decrease. We obtain another necessary condition for stable enveloping grasp

$$a > 1 \tag{16}$$

Figure 4 illustrates the relation between, and θ_2. The color surface represents the potential energy V. The position of the upper globule (point A) represents the initial potential energy in the initial state. Without touching any objects, V decreases as increases. Such motion is a pinching motion, the trajectory of which is represented by the green arrows. If the objects blocks the finger at point B, the pinching motion is stable. The expression of the blue plan is $\theta_1 = \theta_{10}$. The globule which represents the potential energy cannot pass through this plan because the proximal phalanx is blocked by the object.

The color surface and the blue plan intersect in a curve, the red arrow in Fig. 4. After the proximal phalanx touches the object, the potential energy continues

decreasing along the red arrows, which represents an enveloping motion of the PASA-GB finger.

The orange surface represents the state when the distal phalanx touches the objects, which is described in Eq. 10. The globule also cannot pass through the orange plan because the distal phalanx is blocked. The intersection of the color surface, orange surface and blue plan is the potential energy when both phalanges touch the object, which is represented by the lower globule (point C).

In an enveloping grasp, the motion will stop at point C when C is the minimum point of all the possible trajectories. However, once the potential energy V continues decreasing along the blue arrows, the motion will go on and the proximal phalanx will leave the objects until the potential energy reaches the minimum point in the blue arrows. Such motion is called "Ejection motion".

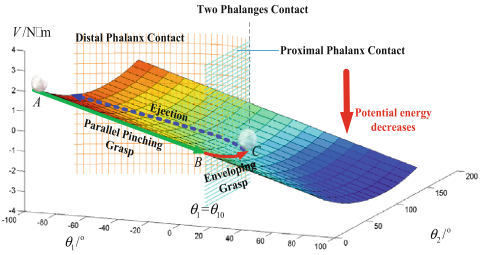

Fig. 4. Potential energy of the PASA-GB finger, where $T = 3\text{N} \cdot \text{m}$, $a = 1.8, M_0 = 0.06\text{N} \cdot \text{m}, k = 0.86\text{N} \cdot \text{m}$, $b = 0.04$ m, $d = 0.03$ m, $R = 0.03$ m, $l_1 = 0.056$ m, $\phi = 0\text{N} \cdot \text{m}$. (Color figure online)

As Fig. 5 shows, the parallel pinching trajectory, enveloping trajectory and ejecting trajectory define a motion zone of the PASA-GB finger. Those three curve are barriers which cannot be passed through. Outside the barriers is a forbidden zone for the PASA-GB finger, which is defined by the position, location and shape of objects.

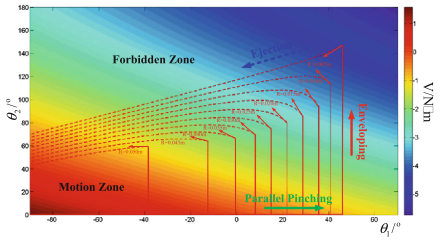

Fig. 5. Motion zone and barrier of the PASA-GB finger, where $T = 3\text{N} \cdot \text{m}$, $a = 1.5$, $M_0 = 0.02\text{N} \cdot \text{m}, k = 0.34\text{N} \cdot \text{m}, b = 0.04$ m, $d = 0.03$ m, $l_1 = 0.056$ m, $\phi = 0\text{N} \cdot \text{m}$.

Another not completely stable grasp happens when the motion stops at an intermediate point of the red arrows in Fig. 4. In order to analyze this case, we need to find out the minimal point of with respect to θ_2:

$$\frac{\partial V}{\partial \theta_2} = 0, \tag{17}$$

$$\theta_{2\,V\min} = (\frac{T}{a} - M_0)/k, \tag{18}$$

As it is shown in Fig. 6a and b, if the horizontal line $\theta_2 = \theta_{2\,V\min}$ across the enveloping trajectory, the enveloping motion will stop at the yellow point as it reaches the minimum value of the potential energy. As a result, the enveloping grasp is not completely stable. To deal with this problem, a and k should not be too large. However, if a is too closed to 1, the ejecting phenomenon will happen, which is shown in Fig. 6d.

Figure 6c shows that a stable grasp is obtained when a and k are proper.

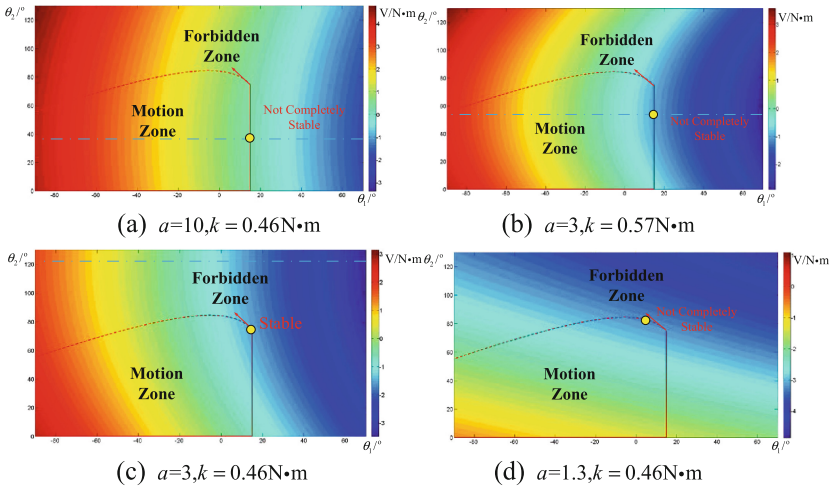

(a) a=10,k = 0.46N•m (b) a=3,k = 0.57N•m

(c) a=3,k = 0.46N•m (d) a=1.3,k = 0.46N•m

Fig. 6. Influence of the transmission ratio and spring force, where $T = 3\text{N} \cdot \text{m}, a = 1.5$, $M_0 = 0.02\text{N} \cdot \text{m}$, $k = 0.34\text{N} \cdot \text{m}$, $b = 0.04$ m, $d = 0.03$ m, $R = 0.03$ m, $l_1 = 0.056$ m, $\phi = 0$ N · m.

3.2 Grasping Forces Analyses

For a stable enveloping grasp, if the contact forces of two phalanges are close, the grasp is tight.

When the grasping motion finishes,

$$[-T, k\theta_2 + M_0]\begin{bmatrix}\delta\beta \\ \delta\theta_2\end{bmatrix} = [\vec{F}_1, \vec{F}_2]\begin{bmatrix}\delta\vec{G}_1^t \\ \delta\vec{G}_2^t\end{bmatrix}, \tag{19}$$

Where

$$[\vec{F}_1, \vec{F}_2]\begin{pmatrix}\delta\vec{G}_1^t \\ \delta\vec{G}_2^t\end{pmatrix} = [F_1, F_2]\begin{bmatrix}-h_1 & 0 \\ -l_1\cos(\theta_2 - \theta_1) & -h_2\end{bmatrix}\begin{bmatrix}\delta\theta_1 \\ \delta\theta_2\end{bmatrix}, \tag{20}$$

$$\begin{pmatrix}\delta\beta \\ \delta\theta_2\end{pmatrix} = \begin{bmatrix}\frac{a-1}{a} & \frac{1}{a} \\ 0 & 1\end{bmatrix}\begin{bmatrix}\delta\theta_1 \\ \delta\theta_2\end{bmatrix}, \tag{21}$$

The relationship among contact forces, driving torque and spring torque is shown as follow:

$$[F_1, F_2] = [-T, k\theta_2 + M_0]\begin{bmatrix}\frac{a-1}{a} & \frac{1}{a} \\ 0 & 1\end{bmatrix}\begin{bmatrix}-h_1 & 0 \\ -l_1\cos(\theta_2 - \theta_1) & -h_2\end{bmatrix}^{-1}. \tag{22}$$

Combine Eqs. 7, 12 and 22, one achieves the final angles of two phalanges and forces distribution based on the position and size of the object, as it is shown in Figs. 7 and 8.

As Fig. 7 shows, $\theta_2 - \theta_1$ becomes larger when the object is closer and larger, which is obviously. Figure 8 shows that the size of objects has much influence on the force distribution. If the object is too large, the contact force of the distal phalanx is much larger than that of the proximal phalanx. Although the finger performs a stable enveloping grasp, the grasp is not so tight. If an unexpected external force is applied on the object, the distal phalanx may be opened and the object will leave the finger. The influence of b shown in Fig. 8 implies that a larger hand base brings better force distribution.

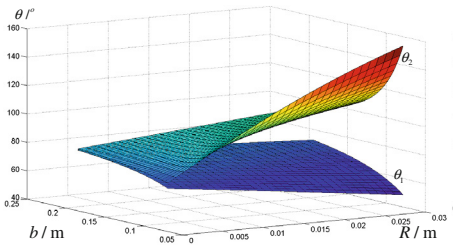

Fig. 7. Rotational angles of the PASA-GB finger.

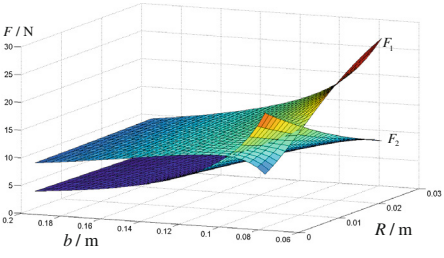

Fig. 8. Force distribution of the PASA-GB finger.

4 Experiments

The prototype of the PASA hand with Gear-belt mechanisms is shown in Fig. 9. It consists of one hand base and three fingers. The motor type is FAULHABER 1616E010.

As it shown in Fig. 9a and b, the PASA hand executes parallel pinching grasp when the bottle is located on the upper side. The Limiting block stops the backward motion of the distal phalanx, which makes the PASA hand pinch objects tightly.

Figure 9c, d and e shows the enveloping motion of the PASA. When the bottle is located on the lower side, the proximal phalanx touches the bottle first. Because of the self-adaptive mechanism, the distal phalanx touches the bottle afterwards.

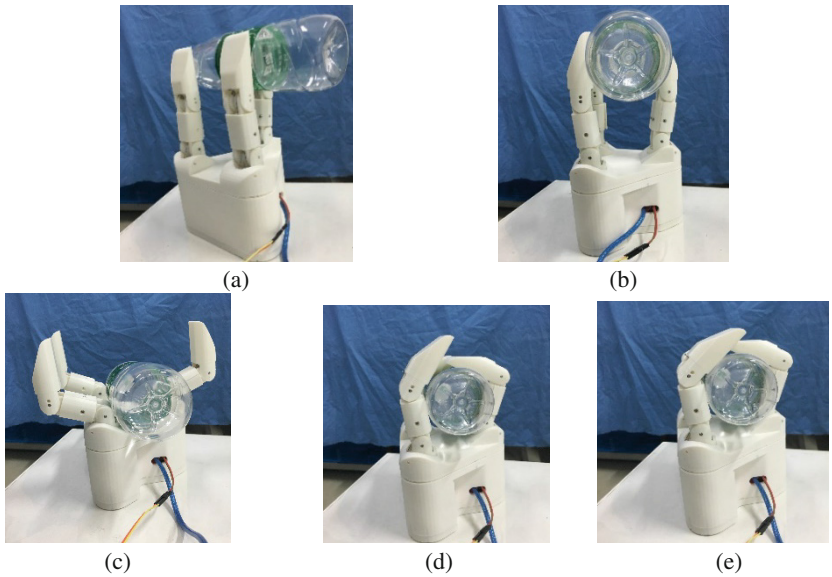

Fig. 9. Experiments of grasping object with the PASA-GB hand.

5 Conclusions

This paper introduces a novel underactuated hand, the PASA-GB hand, which has a hybrid grasping mode. The hybrid grasping mode is a combination of parallel pinching (PA) grasp and self-adaptive enveloping (SA) grasp. Based on the position, size and shape of objects, when the first contact point is located on the lower part of the finger, the finger will execute enveloping grasp. When the first contact is located on the upper part, the finger will execute parallel pinching grasp.

In order to estimate the performance of grasping objects, the potential energy method is used to analyze the stabilities of the PASA-GB hand. The trajectories of pinching grasp, enveloping grasp and ejection form a motion zone for the finger, the

barriers of which are defined by the states of objects. The calculation of force distribution shows the influence of the size and position of objects and provides a method to optimize the force distribution. Experimental results verify the wide adaptability and high practicability of the PASA-GB hand.

Acknowledgement. This Research was supported by National Natural Science Foundation of China (No. 51575302).

References

1. Butterfass, J., Grebenstein, M., Liu, H., et al.: Dlr-hand ii: next generation of a dextrous robot hand. In: Proceedings of the IEEE International Conference on Robotics and Automation, Seoul, Korea, pp. 109–114 (2001)
2. Lovchik, C.S., Diftler, M.A.: The Robonaut hand: a dexterousrobot hand for space. In: Proceedings of the IEEE International Conference on Robotics and Automation (ICRA), pp. 907–912 (1999)
3. Kawasaki, H., Komatsu, T., Uchiyama, K.: Dexterous anthropomorphic robot hand with distributed tactile sensor: Gifu hand II. IEEE/ASME Trans. Mechatron. **7**(3), 296–303 (2002)
4. Bekey, G.A., Tomovic, R., Zeljkovic, I.: Control architecture for the Belgrade/USC hand in dextrous robot hands, pp. 136–149. Springer, New-York (1999)
5. Ueda, J., Ishida, Y., Kondo, M., Ogasawara, T.: Development of the naist-hand with vision-based tactile fingertip sensor. In: Proceedings of the IEEE International Conference on Robotics and Automation, pp. 2343–2348 (2005)
6. Ali, H., Hoi, L.H., Seng, T.C.: Design and development of smart gripper with vision sensor for industrial applications. In: Proceedings of the IEEE International Conference on Computation, pp. 157–180 (2011)
7. Gosselin, C., Laliberte, T., Degoulange, T.: Underactuated robotic hand. In: Video Proceedings of the IEEE International Conference on Robotics and Automation (1998)
8. Lee, S., Noh, S., Lee, Y.K., et al.: Development of bio-mimetic robot hand using parallel mechanisms. In: Proceedings of the IEEE International Conference on Robotics and Biomimetics, pp. 550–555 (2010)
9. de Visser, H., Herder, J.L.: Force-directed design of a voluntary closing hand prosthesis. J. Rehabil. Res. Dev. **37**(3), 261–271 (2000)
10. Bégoc, V., Krut, S., Dombre, E., et al.: Mechanical design of a new pneumatically driven underactuated hand. In: Proceedings of the IEEE International Conference on Robotics and Automation (ICRA), pp. 927–933 (2007)
11. Gaiser, I., Schulz, S., Kargov, A., et al.: A new anthropomorphic robotic hand. In: Proceedings of the IEEE International Conference on Humanoid Robots, pp. 377–386. IEEE (2008)
12. Hirose, S., Umetani, Y.: The developmentof soft gripper for the versatile robot hand. Mech. Mach. Theory **13**, 351–358 (1978)
13. Ciocarlie, M., Allen, P.: Data-driven optimization for underactuated robotic hands. In: Proceedings of the IEEE International Conference on Robotics & Automation, pp. 1292–1299 (2010)
14. Birglen, L., Laliberte, T., Gosselin, C.: Underactuated Robotic Hands. Springer Tracts in Advanced Robotics (2008)

15. Townsend, W.: The BarrettHand grasper – programmably flexible part handling and assembly. Industrial Robot **27**(3), 181–188 (2000)
16. Gosselin, C.M., Laliberte, T.: Underactuated mechanical finger with return actuation, US Patent, US5762390 (1996)
17. Demers, L.A., Lefrancois, S., Jobin, J.: Gripper having a two degree of freedom underactuated mechanical finger for encompassing and pinch grasping, US Patent, US8973958 (2015)
18. Daniel, A.M., Barrett, H., John, U., et al.: Design and testing of aselectively compliant underactuated hand. Int. J. Robot. Res. **33**, 721–735 (2014)
19. Liang, D., Zhang, W., Sun, Z., et al.: PASA finger: a novel parallel and self-adaptive underactuated finger with pinching and enveloping grasp. In: Proceedings of the IEEE International Conference on Robotics and Biomimetics. IEEE (2015)
20. Kragten, G.A.: Underactuated hands: fundamentals, performance analysis and design. Mechanical Maritime & Materials Engineering (2011)